Available online at www.sciencedirect.com

SciVerse ScienceDirect

Ceramics International 39 (2013) 7149–7158

CERAMICS INTERNATIONAL

www.elsevier.com/locate/ceramint

Template free crystallization of zeolite Rho via Hydrothermal synthesis: Effects of synthesis time, synthesis temperature, water content and alkalinity

Seyed Foad Mousavi, Mostafa Jafari, Mansoor Kazemimoghadam, Toraj Mohammadi*

Research Centre for Membrane Separation Processes, Faculty of Chemical Engineering, Iran University of Science and Technology (IUST), Narmak, Tehran, Iran

Received 15 January 2013; received in revised form 18 February 2013; accepted 18 February 2013
Available online 4 March 2013

Abstract

Four parameters affecting organic template free hydrothermal synthesis of Rho zeolite were investigated, including synthesis time, synthesis temperature, water content, and alkalinity. XRD and SEM techniques were applied to characterize the synthesized zeolite Rho powders. The results showed that synthesis time has a higher impact on the crystal size. The crystal size increases from 1.45 to 1.90 μm by increasing synthesis time from 4 to 10 days. Synthesis time is also effective on the crystals morphology and there is an extremum in the diagram of crystallinity versus synthesis time for zeolite Rho. In addition, synthesis temperature has high impact on morphology of the crystals and can change the zeolite phases. Besides, water content is also highly effective on crystallinity of the synthesized powders and with increasing water content the crystallinity decreases dramatically. At last, increasing alkalinity increases the nucleation and decreases the crystals size. At water content of 400 mol, pollucite phase was synthesized at two ratios of $Na_2O/Al_2O_3=6$ and $Cs_2O/Al_2O_3=0.8$, and also two ratios of $Na_2O/Al_2O_3=9$ and $Cs_2O/Al_2O_3=1.2$; and for these ratios the mean crystal sizes were 0.70 and 0.40 μm, respectively, confirming the negative effect of alkalinity on the mean crystal size.

Keywords: Zeolite Rho; Synthesis time and temperature; Template free; Water content; Alkalinity

1. Introduction

Zeolites are crystalline aluminosilicates with three-dimensional framework structure that form uniformly sized pores of molecular dimensions. Their pores preferentially adsorb molecules that fit snugly inside them and exclude molecules that are larger, they act as sieves on a molecular scale. Thus, zeolites are a subset of molecular sieves. Using molecular sieves with three-dimensional framework structures is well entrenched in applications as diverse as laundry detergents [1,2], catalysts [3–5], adsorbents [6–8], gas separations [9–11], pervaporation [12–15], membrane reactors [16–18], ion exchange [19–21], agriculture and horticulture [22,23], and is finding new applications in electronics [24], magnetism [25,26], chemical sensors [27–29], medicine [30], etc. [31–33]. Zeolites are typically synthesized under hydrothermal conditions from alkaline aqueous solutions. However, they are difficult to be analyzed in situ because the hydrothermal treatment involves high temperatures and pressures [34]. A typical hydrothermal zeolite synthesis can be described in briefest terms as follows: (1) amorphous reactants containing silica and alumina are mixed together with a cation source, usually in a basic (high pH) medium. (2) The aqueous reaction mixture is heated, often in a sealed autoclave. (3) For a period at synthesis temperature, the reactants remain amorphous. (4) After the above "induction period", the crystalline zeolite products are formed. (5) Gradually, most amorphous materials are replaced by an approximately equal mass of the zeolite crystals [35].

Zeolite Rho is known as a zeolite with a flexible and collapsible framework structure, meaning that the framework is able to adapt to different size cations and differently shaped adsorbed molecules [36]. Zeolite Rho is a small pore

*Corresponding author. Tel.: +98 21 789 6621; fax: +98 21 789 6620.
E-mail address: torajmohammadi@iust.ac.ir (T. Mohammadi).

0272-8842/$ - see front matter © 2013 Elsevier Ltd and Techna Group S.r.l. All rights reserved.
http://dx.doi.org/10.1016/j.ceramint.2013.02.058

size zeolite, 3.6×3.6 Å with a low Si/Al ratio (2.5–3.0) [37]. The framework of zeolite Rho is composed of a body-centered cubic arrangement of truncated cubo-octahedra or α-cages linked via double 8-rings of silicon and aluminumtetrahedral as shown in Fig. 1 [38,39].

There are some parameters that affect synthesis of zeolites. Synthesis time can affect zeolite phases, morphology and crystallinity. Temperature is the other most important factor in the synthesis of zeolites. All researchers paid particular attention to the crystallization temperature due to its significant effect on zeolites synthesis. The desired zeolite phases typically can only be obtained within a specific temperature range. Temperature does not only affect the crystal size, but also the crystal morphology [40].

A general principle states that the crystal growth rate is proportional to concentration of reactants, as expressed by the concentration function $f(C)$, that is

$$dL/dt_c = k_g f(C),$$

where L is the length of synthesized crystals, t_c is the crystallization time and k_g is the growth rate. It is expected that dilution of the crystallizing system (e.g., increasing water content) reduces the concentration of reactive species in liquid phase, and thus decreases the crystal growth rate. The observed influence of the concentration on the crystal growth rate is caused by the fact that the growth condition is mainly characterized by the supersaturation of the primary building units for the crystallization [41].

Increasing alkalinity has also a major impact on the number and the morphology of crystals [42]. Ren et al. concluded that alkalinity has a great influence on the Si/Al molar ratio of the product via controlling the dissolution rate of amorphous silica and aluminum hydroxide in the synthesis of zeolite ZSM-5 crystals [43].

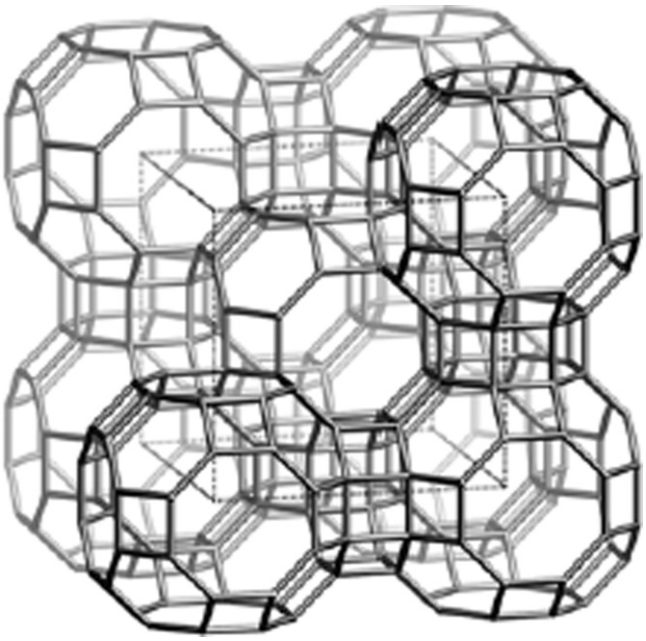

Fig. 1. Schematic view of Rho zeolite framework.

To obtain highly crystallized zeolites, particular organic templates are usually necessary to be used as structure directing and charge balancing agents. However, there are obvious disadvantages for organic template-contained synthesis, such as their relatively high cost and environmental pollution impacts [44–46]. For these reasons, it is better to avoid using organic templates in zeolites synthesis gels for industrialization.

In most previous works in the field of zeolite Rho synthesis, organic templates were used as structure directing agents (SDA) [34,40,47]. In this study, we tried to synthesize template free zeolite Rho and investigate the effects of some parameters including synthesis time, synthesis temperature, water content of gel formula, and alkalinity.

2. Experimental

2.1. Zeolite synthesis

Materials used for synthesis of the zeolite powders were sodium aluminate (Riedel-de Haë]n, 53 wt%) as Al source, LUDOX (Aldrich, 40 wt% suspension in water) as Si source, cesium hydroxide (Alfa Aesar, 50 wt% aqueous solution) as cation, sodium hydroxide (pellets, Merck, 97 wt%) as cation and deionized water.

In order to investigate the effects of synthesis time, synthesis temperature, alkalinity and water content, nine gels were prepared. Table 1 shows gel formulas of the synthesized powders with their synthesis time and temperature. The gels were prepared via the hydrothermal synthesis method without using any template. For the synthesis, some parameters were kept constant. They were SiO_2/Al_2O_3, Na_2O/Al_2O_3, stirrer speed, aging time, and aging temperature that were 10.8, 3, 1000 rpm, 24 h, and 25 °C, respectively.

The method used for preparing all the gel mixtures was the same. At first, a certain amount of sodium hydroxide was added to deionized water and the mixture was stirred for 10 min for complete dissolving. While stirring, a sufficient amount of cesium hydroxide according to the gel formula was added to the solution. Then sodium aluminate was added to the solution and was stirred for another 10 min. After that, a sufficient amount of LUDOX was added to the solution and after covering the stirring solution by nylon in order to prevent water loss, the gel was stirred for 1 day at ambient temperature (approximately 25 °C). Then, the prepared gels were poured into PTFE autoclaves for heating according to their synthesis times as shown in Table 1. The products were washed with double ionized water until the pH was less than 9 and then dried at 100 °C.

After heating, all the gels were filtered using filter paper and washed by deionized water, while a vacuum pump was

Table 1
Gel formulas and preparing conditions of synthesized powders.

Synthesis number	Gel composition					Crystallization conditions	
	Al_2O_3	Na_2O	Cs_2O	SiO_2	H_2O	Synthesis time (days)	Temperature (°C)
1	1	3	0.4	10.8	110	4	100
2	1	3	0.4	10.8	110	7	100
3	1	3	0.4	10.8	110	10	100
4	1	3	0.4	10.8	110	7	80
5	1	3	0.4	10.8	110	7	120
6	1	3	0.4	10.8	200	7	100
7	1	3	0.4	10.8	400	7	100
8	1	6	0.8	10.8	400	7	100
9	1	9	1.2	10.8	400	7	100

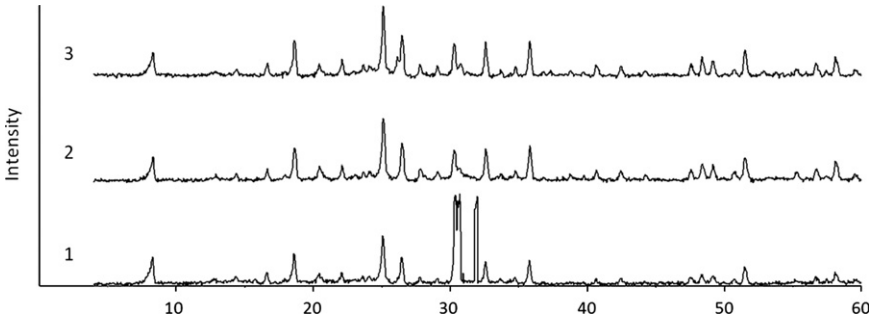

Fig. 2. XRD patterns of the synthesized gels of 1, 2 and 3 (synthesis time of 4, 7 and 10 days, respectively).

applied. At the end, all the filtered powders were dried at 80 °C for 2 h.

2.2. Zeolite characterization

The zeolite crystals were characterized by X-ray diffraction (XRD) using an X-ray diffractometer (SIEMENS, D5000, 1500 W, 35 kV, 20 mA) with Cu radiation, with a 2θ range of 4–60°. Morphology of the crystals was examined by Scanning Electron Microscopy (SEM) using a scanning electron microscope (JEM-1200 or JEM-5600LV equipped with an Oxford ISIS-300 X-ray disperse spectroscopy (EDS)).

XRD patterns of the produced powders were analyzed with the aid of Xpowder (version 2004). SEM images were also analyzed with the aid of Microstructure Measurement software in order to obtain the mean size of the crystals. Scherrer numbers were also determined using the following equation:

$$\tau = \frac{K\lambda}{\beta \cos\theta}$$

where K is the shape factor, λ is the X-ray wavelength, β is the line broadening at half the maximum intensity (FWHM) in radians, and θ is the Bragg angle.

3. Results and discussion

3.1. Effect of synthesis time

Fig. 2 shows XRD patterns of the synthesis gel synthesized for 4, 7 and 10 days (samples of 1–3) according to Table 1. In comparison with standard diffraction data of zeolite Rho (JCPDS card number 39-1366), the results of XRD patterns indicate that the zeolite Rho crystals are formed from the synthesis gels, while the maximum degree of crystallinities is observed for 7 days of synthesis. It means that 7 days of synthesis is the best synthesis time among these three examined time intervals for the synthesis gel. It also indicates that no phase change occurs in this time interval, as presented by Park et al. [48].

Applying the Scherrer equation, crystal sizes for the synthesized samples of 1, 2, and 3 were calculated as 25, 28, and 34 nm, respectively, showing the positive effect of synthesis time on crystal growth.

Fig. 3 shows SEM images of these three samples. From the microstructure measurement software analysis, the mean crystal sizes of the samples 1, 2, and 3 were measured approximately as 1.45, 1.70 and 1.90 μm, respectively, confirming the positive effect of synthesis time on the zeolite Rho crystal growth as presented by Araki et al. [34] and Liu et al. [49]. Araki et al. pointed to a four step zeolite Rho synthesis mechanism: (1) formation of

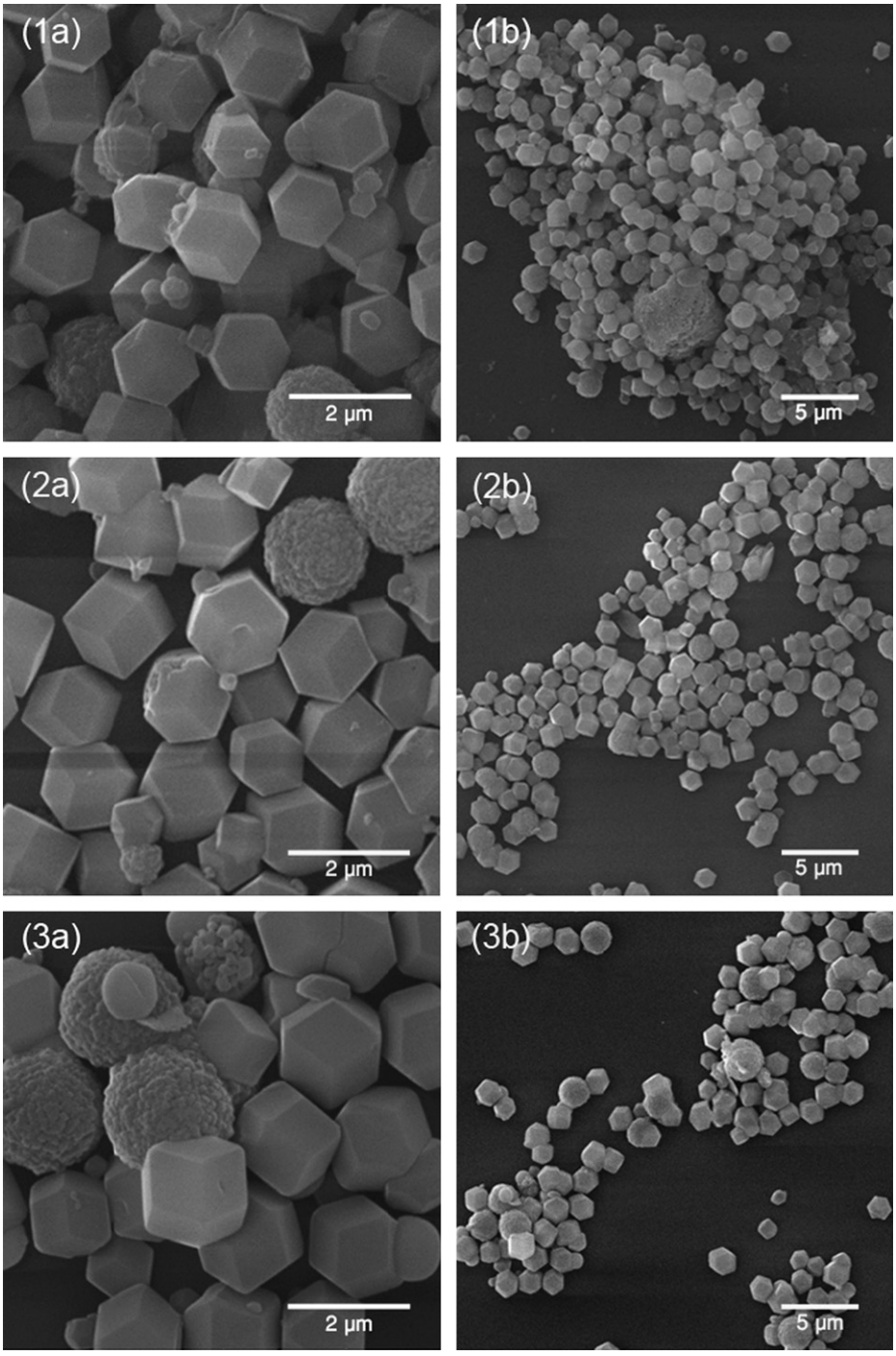

Fig. 3. SEM images of samples 1–3.

aluminosilicates, (2) particle growth and aggregation, (3) crystallization and crystal growth and (4) gentle crystal growth. The SEM images demonstrate the last three steps of the synthesis mechanism. In this figure, it is clear that two phases are formed: geometric form of zeolite Rho and amorphous aggregates. As observed, some crystals are half-formed and their other half is non-formed amorphous aggregates. It seems that the aggregates are going to convert to the crystals, according to the fourth step. It is also clear that size distribution of the particles is getting narrower with increasing synthesis time. This may be due to the fact that the crystals are being formed and are growing, and the particles are converting to the crystals as synthesis time goes on [34].

3.2. Effect of synthesis temperature

Fig. 4 shows XRD patterns of the synthesis gel synthesized at 100, 80 and 120 °C (samples 2, 4 and 5, respectively) according to Table 1. The results of XRD patterns

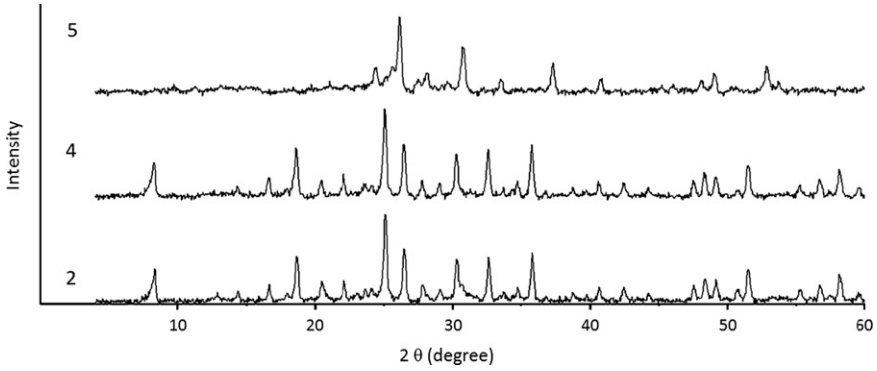

Fig. 4. XRD patterns of the synthesized gel of 2, 4 and 5 (synthesis temperature of 100, 80 and 120 °C, respectively).

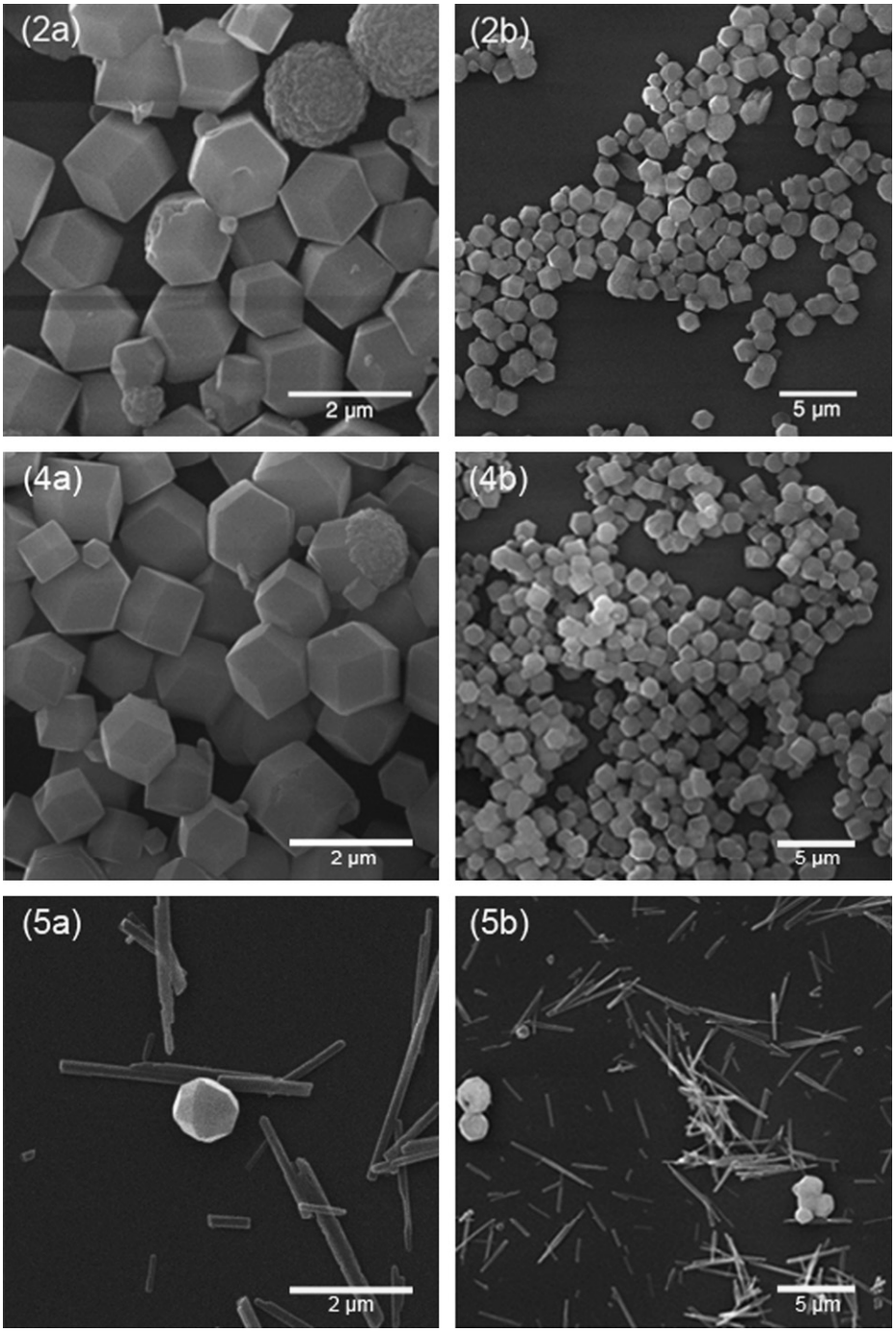

Fig. 5. SEM images of samples 2, 4, and 5.

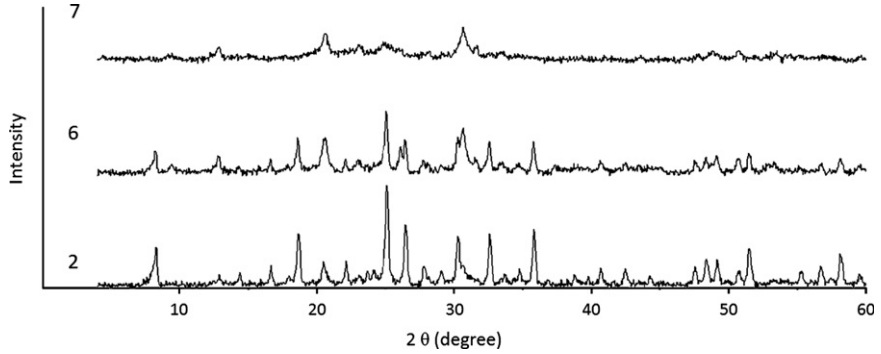

Fig. 6. XRD patterns of the synthesized gels of 2, 6 and 7 (synthesis gel water content of 110, 200 and 400 mol, respectively).

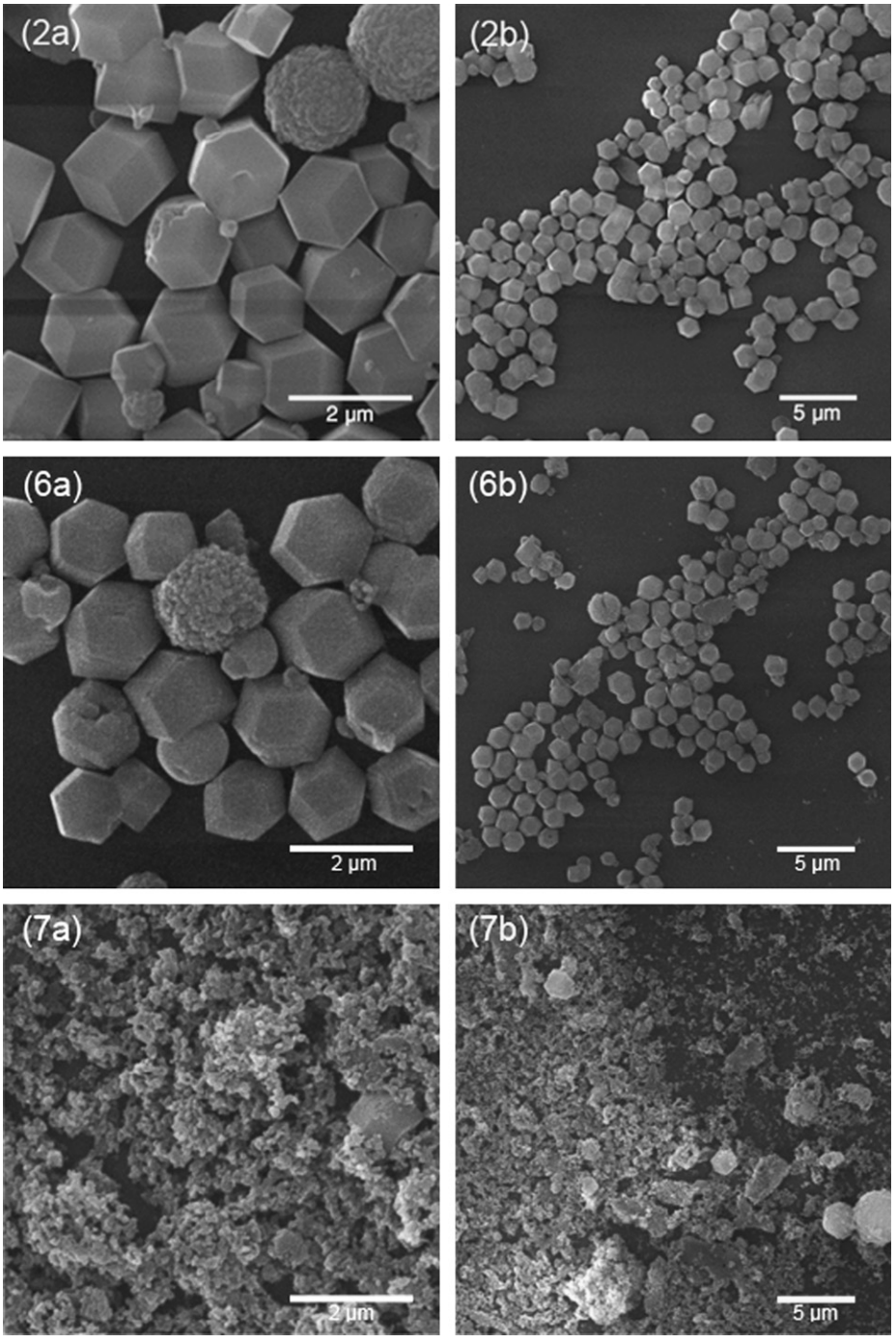

Fig. 7. SEM images of samples 2, 6, and 7.

indicate that zeolite Rho crystals are formed at synthesis temperatures of 80 °C and 100 °C (samples 2 and 4, respectively), and pollucite phase is formed at 120 °C (sample 5). The results show that sample 2 at a synthesis temperature of 100 °C exhibits slightly sharper peaks and more intensity and therefore has slightly more crystallinity than sample 4 at a synthesis temperature of 80 °C; this is similar to the results reported by Mehdipourghazi et al. regarding nano-size MFI zeolite [50]. At synthesis temperature of 120 °C (sample 5), the phase is changed confirming that at this synthesis temperature and synthesis time, zeolite Rho crystals cannot be formed. So, it can be said that synthesis temperature of 120 °C is higher than the temperature needed to form Rho zeolite crystals for 7 days of synthesis.

Fig. 5 shows SEM images of these three samples. From the SEM images, it can be observed that crystals size in sample 2 synthesized at 100 °C is greater than that in sample 4 synthesized at 80 °C. The mean crystal size of sample 2 is approximately 1.70 μm, while that of sample 4 is 1.40 μm confirming that synthesis temperature has a negligible positive effect on the crystal size, as reported by Mehdipourghazi et al. [50].

However, at 120 °C, the results show that synthesis temperature significantly affects phases of the synthesized zeolite crystals.

Murayama et al. investigated the effect of reaction temperature on hydrothermal synthesis of potassium type zeolites from coal fly ash and presented that the higher the reaction temperature in the range from 393 K to 453 K, the higher the reaction rate [51].

3.3. Effect of water content

Fig. 6 shows XRD patterns of the synthesis gels synthesized using water content of 110, 200 and 400 mol (2, 6 and 7, respectively) according to Table 1. The results of XRD patterns indicate that zeolite Rho crystals are formed using water content of 110 and 200 mol (samples 2 and 6) and a little is formed using water content of 400 mol (sample 7). The XRD results show that sample 7 has some same peaks of Rho crystals but not all of them. Fig. 7 shows that there are less zeolite (Rho) crystals and more amorphous phase. The results confirm that this degree of concentration is not enough for the synthesis of zeolite Rho crystals.

Applying the Scherrer equation, crystals sizes for the synthesized samples of 2 and 6 were calculated as 28 and 17 nm, respectively.

Fig. 7 shows SEM images of these three samples. From the microstructure measurement software analysis, the mean crystal sizes of the samples 2, 6, and 7 were measured approximately as 1.70, 1.30, 1.15 μm, respectively, confirming the negative effect of water content on the crystal growth.

It is clear that the formation of zeolite crystals depends on the amount of supersaturation in gel. When water content in the gel increases, supersaturation and consequently nucleation and crystal growth decrease and this thus reduces crystallinity and the crystals become smaller at the same synthesis time and temperature. By adding more water to the gel, the supersaturation is missed in the gel and therefore crystallization is stopped. According to the results reported by Araki et al. [34], the products may already exist in steps 2 and 3 (particle growth and aggregation, and crystallization and crystal growth). So by further extending synthesis time using water content of 400, zeolite Rho with higher crystallinity may be formed; according to Fig. 7(a and b), there are aluminosilicate particles and aggregates, and crystals are being formed.

3.4. Effect of alkalinity

It was finally decided to investigate the effect of alkalinity in the synthesis gel at water content of 400 mol in order to obtain zeolite Rho phase at low concentration. As observed in Table 1, sample 8 ($Na_2O/Al_2O_3=6$ and $Cs_2O/Al_2O_3=0.8$) has two times higher alkalinity than

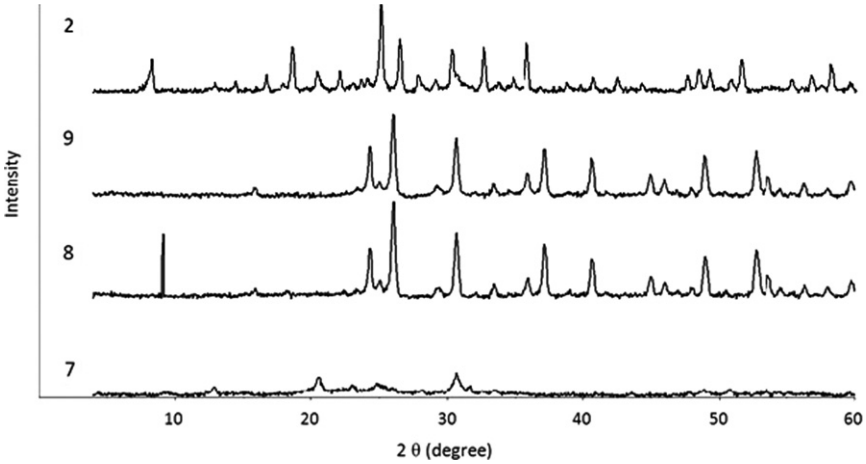

Fig. 8. XRD patterns of the synthesized gels of 7, 8, 9 and 2 (alkalinity ratio to sample 7 of 1, 2, 3 and 1 respectively).

sample 7 ($Na_2O/Al_2O_3=3$ and $Cs_2O/Al_2O_3=0.4$) and sample 9 ($Na_2O/Al_2O_3=9$ and $Cs_2O/Al_2O_3=1.2$) has three times higher alkalinity than sample 7. From samples 7 to 9, the total amorphous phase (sample 7) is approximately changed to the total crystalline pollucite phase (samples 8 and 9). From XRD analysis and SEM images (Figs. 8 and 9), it is clear that increasing alkalinity (from samples 8 to 9), the crystallinity increases and the crystals size decreases. It means that with increasing alkalinity, more amorphous phase is converted to the pollucite phase.

As observed, alkalinity has a negative effect on the crystal size. The mean crystal size in sample 8 is 0.70 and in sample 9 is 0.40 μm approximately, showing that the crystal size decreases dramatically with increasing alkalinity.

It can be concluded that by increasing alkalinity, crystals size decreases and nucleation increases. Torres et al. also investigated the influence of gel alkalinity on the synthesis and physicochemical properties of zeolite [Ti,Al]-Beta and concluded that the smaller zeolite particles are obtained for the samples crystallized from the more alkaline gels [52].

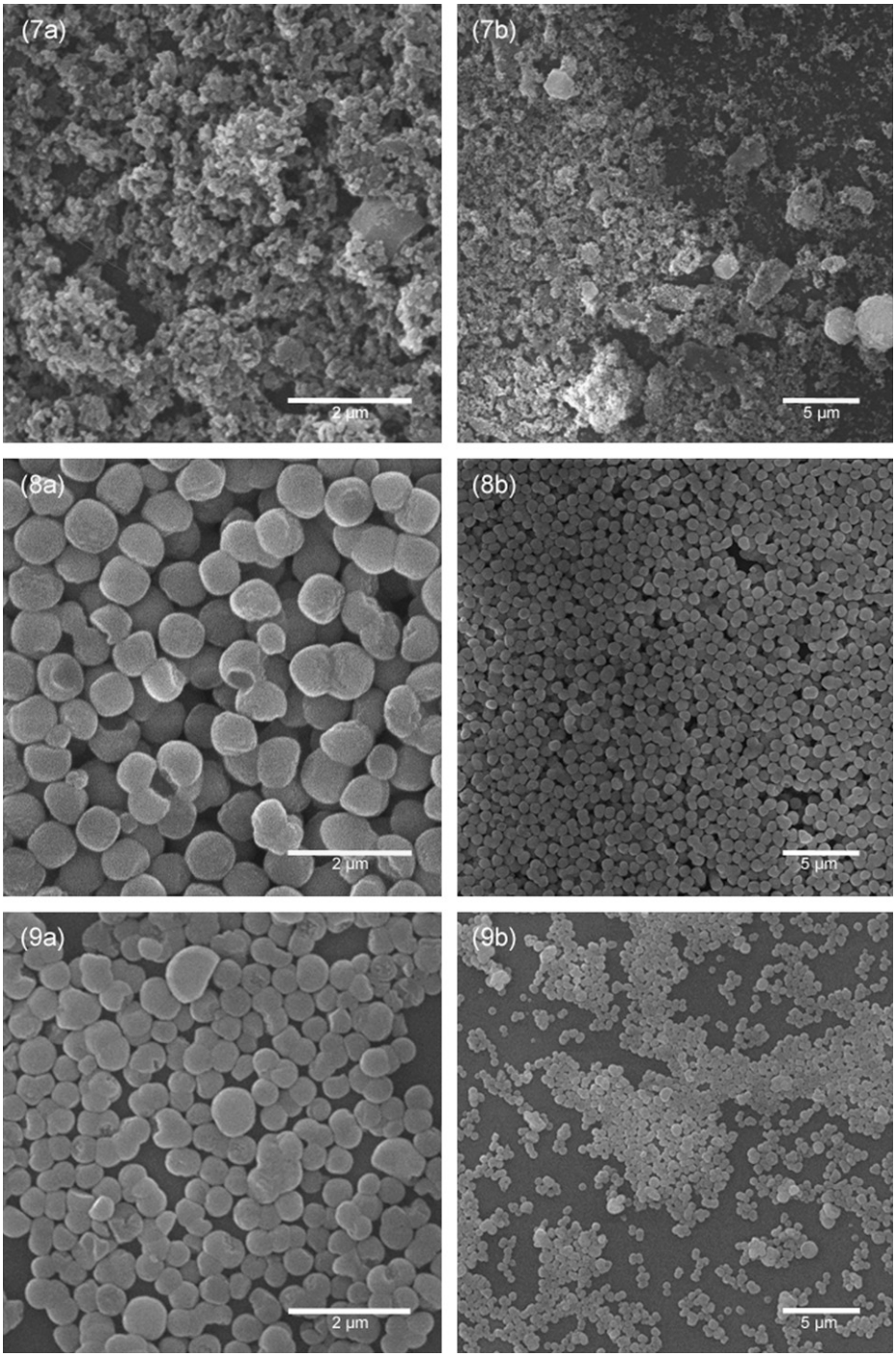

Fig. 9. SEM images of samples 7, 8, and 9.

4. Conclusion

The main purpose of this research was to investigate the effects of different parameters on template free synthesis of zeolite Rho, including synthesis time, synthesis temperature, water content and alkalinity. From the XRD patterns and SEM images, it was concluded that longer synthesis time affects the crystals size dramatically. The crystal size increases from 1.45 to 1.90 μm by increasing synthesis time from 4 to 10 days. Synthesis time also affects the crystals morphology and from the results of this work, there should be an extremum in the diagram of crystallinity versus synthesis time for the formation of zeolite Rho. In addition, synthesis temperature is effective on morphology of the crystals and can change the crystals phase. Moreover, water content is effective on crystallinity of the synthesized zeolite and increasing water content decreases the crystallinity dramatically. Increasing alkalinity of the gel increases the nucleation and also decreases the crystals size. With increasing alkalinity at water content of 400 mol, pollucite crystals are obtained. At $Na_2O/Al_2O_3=6$ and $Cs_2O/Al_2O_3=0.8$ ratios, the mean crystal size is 0.70 and at $Na_2O/Al_2O_3=9$ and $Cs_2O/Al_2O_3=1.2$ ratios, it is 0.40 μm approximately, showing the negative effect of alkalinity on the mean crystal size.

Acknowledgments

This research was supported by the National Iranian Gas Company (NIGC).

References

[1] K.S. Hui, C.Y.H. Chao, Pure, single phase, high crystalline, chamfered-edge zeolite 4A synthesized from coal fly ash for use as a builder in detergents, Journal of Hazardous Materials 137 (1) (2006) 401–409.
[2] H. Upadek, E. Smulders, J. Poethkow, Laundry detergent additive containing zeolite, polycarboxylate, and perborate, Zeolites 11 (1) (1991) 90.
[3] V. Kanazirev, T. Tsoncheva, Reaction pathways of methanol over Pt/zeolite catalysts: effect of different active sites, Zeolites 9 (6) (1989) 516–520.
[4] P. Liu, J. Wang, X. Zhang, R. Wei, X. Ren, Catalytic performances of dealuminated Hβ zeolite supported Pt catalysts doped with Cr in hydroisomerization of n-heptane, Chemical Engineering Journal 148 (1) (2009) 184–190.
[5] J. Varga, J. Halász, I. Kiricsi, Modified ZSM-5 zeolite as DENOX catalyst, Environmental Pollution 102 (1) (1998) 691–695.
[6] Z. Zhao, X. Cui, J. Ma, R. Li, Adsorption of carbon dioxide on alkali-modified zeolite 13X adsorbents, International Journal of Greenhouse Gas Control 1 (3) (2007) 355–359.
[7] L. Damjanović, V. Rakić, V. Rac, D. Stošić, A. Auroux, The investigation of phenol removal from aqueous solutions by zeolites as solid adsorbents, Journal of Hazardous Materials 184 (1–3) (2010) 477–484.
[8] I. Ali Khan, K.F. Loughlin, Kinetics of sorption in deactivated zeolite crystal adsorbents, Computers and Chemical Engineering 27 (5) (2003) 689–696.
[9] M.W. Ackley, S.U. Rege, H. Saxena, Application of natural zeolites in the purification and separation of gases, Microporous and Mesoporous Materials 61 (1–3) (2003) 25–42.
[10] P. Vareltzis, E.S. Kikkinides, M.C. Georgiadis, On the optimization of gas separation processes using zeolite membranes, Chemical Engineering Research and Design 81 (5) (2003) 525–536.
[11] T. Tomita, K. Nakayama, H. Sakai, Gas separation characteristics of DDR type zeolite membrane, Microporous and Mesoporous Materials 68 (1–3) (2004) 71–75.
[12] T.C. Bowen, R.D. Noble, J.L. Falconer, Fundamentals and applications of pervaporation through zeolite membranes, Journal of Membrane Science 245 (1–2) (2004) 1–33.
[13] G. Li, E. Kikuchi, M. Matsukata, A study on the pervaporation of water–acetic acid mixtures through ZSM-5 zeolite membranes, Journal of Membrane Science 218 (1–2) (2003) 185–194.
[14] C. Yu, C. Zhong, Y. Liu, X. Gu, G. Yang, W. Xing, N. Xu, Pervaporation dehydration of ethylene glycol by NaA zeolite membranes, Chemical Engineering Research and Design 90 (9) (2012) 1372–1380.
[15] S.-L. Wee, C.-T. Tye, S. Bhatia, Membrane separation process—pervaporation through zeolite membrane, Separation and Purification Technology 63 (3) (2008) 500–516.
[16] B.-H. Jeong, K.-I. Sotowa, K. Kusakabe, Catalytic dehydrogenation of cyclohexane in an FAU-type zeolite membrane reactor, Journal of Membrane Science 224 (1–2) (2003) 151–158.
[17] Y. Zhang, Z. Wu, Z. Hong, X. Gu, N. Xu, Hydrogen-selective zeolite membrane reactor for low temperature water gas shift reaction, Chemical Engineering Journal 197 (0) (2012) 314–321.
[18] J. van den Bergh, C. Gücüyener, J. Gascon, F. Kapteijn, Isobutane dehydrogenation in a DD3R zeolite membrane reactor, Chemical Engineering Journal 166 (1) (2011) 368–377.
[19] T.C. Watling, L.V.C. Rees, Ion exchange in zeolite EU-1: Part 2. The effect of the chemical nature of the exchange site, Zeolites 14 (8) (1994) 693–696.
[20] J. Hou, J. Yuan, R. Shang, Synthesis and characterization of zeolite W and its ion-exchange properties to K+ in seawater, Powder Technology 226 (0) (2012) 222–224.
[21] R.M. Mohamed, A.A. Ismail, G. Kini, I.A. Ibrahim, B. Koopman, Synthesis of highly ordered cubic zeolite A and its ion-exchange behavior, Colloids and Surfaces A: Physicochemical and Engineering Aspects 348 (1–3) (2009) 87–92.
[22] K. Ramesh, D.D. Reddy, Chapter four—zeolites and their potential uses in agriculture, in: L.S. Donald (Ed.), Advances in Agronomy, Vol. 113, Academic Press, 2011, pp. 219–241.
[23] W. Chesworth, P. Van Straaten, P. Smith, S. Sadura, Solubility of apatite in clay and zeolite bearing systems: application to agriculture, Applied Clay Science 2 (3) (1987) 291–297.
[24] O.H. Elsayed-Ali, T. Abdel-Fattah, H.E. Elsayed-Ali, Copper cation removal in an electrokinetic cell containing zeolite, Journal of Hazardous Materials 185 (2–3) (2011) 1550–1557.
[25] J.-L. Cao, X.-W. Liu, R. Fu, Z.-Y. Tan, Magnetic P zeolites: synthesis, characterization and the behavior in potassium extraction from seawater, Separation and Purification Technology 63 (1) (2008) 92–100.
[26] P.G. Bercoff, H.R. Bertorello, C. Saux, L.B. Pierella, P.M. Botta, T. Kanazawa, Y. Zhang, Magnetic properties of Co-impregnated zeolites, Journal of Magnetism and Magnetic Materials 321 (22) (2009) 3813–3820.
[27] T. Baimpos, L. Gora, V. Nikolakis, D. Kouzoudis, Selective detection of hazardous VOCs using zeolite/Metglas composite sensors, Sensors and Actuators A: Physical 186 (0) (2012) 21–31.
[28] A. Dubbe, The effect of platinum clusters in the zeolite micropores of a zeolite-based potentiometric hydrocarbon gas sensor, Sensors and Actuators B: Chemical 137 (1) (2009) 205–208.
[29] P. Varsani, A. Afonja, D.E. Williams, I.P. Parkin, R. Binions, Zeolite-modified WO_3 gas sensors—Enhanced detection of NO_2, Sensors and Actuators B: Chemical 160 (1) (2011) 475–482.
[30] G. Cerri, M. de' Gennaro, M.C. Bonferoni, C. Caramella, Zeolites in biomedical application: Zn-exchanged clinoptilolite-rich rock as

active carrier for antibiotics in anti-acne topical therapy, Applied Clay Science 27 (3–4) (2004) 141–150.
[31] E.M.F.H. van Bekkum, P.A. Jacobs, J.C. Jansen, Introduction to Zeolite Science and Practice, Elsevier, 2001.
[32] P.K.D.P. Payra, Handbook of Zeolite Science and Technology, Marcel Dekker, Inc., New York, Basel, 2003.
[33] J. Yu, Synthesis of zeolites, in: B.A.C. Jiří Čejka, S. Ferdi (Eds.), Studies in Surface Science and Catalysis, Vol. 168, Elsevier, 2007, pp. 39–103 (Chapter 3).
[34] S. Araki, Y. Kiyohara, S. Tanaka, Y. Miyake, Crystallization process of zeolite rho prepared by hydrothermal synthesis using 18-crown-6 ether as organic template, Journal of Colloid and Interface Science 376 (1) (2012) 28–33.
[35] C.S. Cundy, P.A. Cox, The hydrothermal synthesis of zeolites: precursors, intermediates and reaction mechanism, Microporous and Mesoporous Materials 82 (1–2) (2005) 1–78.
[36] A. Bieniok, K.D. Hammonds, Rigid unit modes and the phase transition and structural distortions of zeolite rho, Microporous and Mesoporous Materials 25 (1–3) (1998) 193–200.
[37] L.J. Garces, V.D. Makwana, B. Hincapie, A. Sacco, S.L. Suib, Selective N,N-methylation of aniline over cocrystallized zeolites RHO and zeolite X (FAU) and over Linde type L (Sr,K-LTL), Journal of Catalysis 217 (1) (2003) 107–116.
[38] D.R. Corbin, L. Abrams, G.A. Jones, R.L. Harlow, P.J. Dunn, Flexibility of the zeolite RHO framework: effect of dehydration on the crystal structure of the beryllophosphate mineral, pahasapaite, Zeolites 11 (4) (1991) 364–367.
[39] J.B. Parise, E. Prince, The structure of cesium-exchanged zeolite-RhO at 293 K and 493 K determined from high resolution neutron powder data, Materials Research Bulletin 18 (7) (1983) 841–852.
[40] S. Liu, P. Zhang, X. Meng, D. Liang, N. Xiao, F.-S. Xiao, Cesium-free synthesis of aluminosilicate RHO zeolite in the presence of cationic polymer, Microporous and Mesoporous Materials 132 (3) (2010) 352–356.
[41] J. Bronić, Handbook of Zeolite Science and Technology, Theoretical and Practical Aspects of Zeolite Crystal Growth, Zagreb, Croatia, 2003.
[42] J. Bronić, A. Palčić, B. Subotić, L. Itani, V. Valtchev, Influence of alkalinity of the starting system on size and morphology of the zeolite A crystals, Materials Chemistry and Physics 132 (2–3) (2012) 973–976.
[43] N. Ren, J. Bronić, B. Subotić, X.-C. Lv, Z.-J. Yang, Y. Tang, Controllable and SDA-free synthesis of sub-micrometer sized zeolite ZSM-5. Part 1: influence of alkalinity on the structural, particulate and chemical properties of the products, Microporous and Mesoporous Materials 139 (1–3) (2011) 197–206.
[44] L. Zhang, S. Liu, S. Xie, L. Xu, Organic template-free synthesis of ZSM-5/ZSM-11 co-crystalline zeolite, Microporous and Mesoporous Materials 147 (1) (2012) 117–126.
[45] X. Huang, Z. Wang, Synthesis of zeolite Zsm-5 small particle aggregates by a two-step method in the absence of an organic template, Chinese Journal of Catalysis 32 (11–12) (2011) 1702–1711.
[46] K.P. Dey, S. Ghosh, M.K. Naskar, Organic template-free synthesis of ZSM-5 zeolite particles using rice husk ash as silica source, Ceramics International 39 (2) (2013) 2153–2157.
[47] P. Feng, X. Bu, G.D. Stucky, Amine-templated syntheses and crystal structures of zeolite rho analogs, Microporous and Mesoporous Materials 23 (5–6) (1998) 315–322.
[48] M. Park, S. Kim, N. Heo, S. Komarneni, Synthesis of zeolite rho: aging temperature effect, Journal of Porous Materials 3 (3) (1996) 151–155.
[49] X. Liu, X. Zhang, X. Tan, Z. Chen, Hydrothermal synthesis of zeolite Rho using methylcellulose as the space-confinement additive, Ceramics International, in press.
[50] M. Mehdipourghazi, A. Moheb, H. Kazemian, Incorporation of boron into nano-size MFI zeolite structure using a novel microwave-assisted two-stage varying temperatures hydrothermal synthesis, Microporous and Mesoporous Materials 136 (1–3) (2010) 18–24.
[51] N. Murayama, T. Takahashi, K. Shuku, H.-HPlease check the author's initials in Ref. [51] and correct if necessary.. Lee, J. Shibata, Effect of reaction temperature on hydrothermal syntheses of potassium type zeolites from coal fly ash, International Journal of Mineral Processing 87 (3–4) (2008) 129–133.
[52] J.C. Torres, D. Cardoso, The influence of gel alkalinity in the synthesis and physicochemical properties of the zeolite [Ti,Al]-Beta, Microporous and Mesoporous Materials 113 (1–3) (2008) 204–211.